NUMERICAL ASSESSMENT OF COMBUSTION PARAMETERS ON THERMAL REGENERATIVE LADLE PREHEATING

Lipeng WANG, Tao CHI, Xuebo CHEN*

[*]School of Electronic and Information Engineering, University of Science and Technology Liaoning, Anshan 114051, China

[*] Corresponding author; E-mail: xuebochen@126.com

Ladle preheating, as a crucial component of steel production, exerts a notable influence on both energy consumption and NOx emission levels throughout the entire production process. To investigate the impact of the excess air coefficient on the preheating process of the regenerative ladle, this paper firstly adopts numerical simulation method; a multi-field coupled mathematical model is established for simulating the gas combustion, flow, and coupled heat transfer within the thermal storage ladle. This approach is grounded in the standard k-ε turbulence model, the component transport combustion model, and the DO radiation model. Subsequently, using the finite element analysis software ANSYS Fluent 2024 R1, simulations was conducted for the combustion fields inside the ladle at various excess air coefficients (0.9, 0.95, 1, 1.05, 1.1, 1.15, and 1.2) based on the established model. For each excess air coefficient, the flow field, temperature field, and NOx distribution within the ladle were analyzed. The results indicate that, under the specified boundary conditions, both excessively high and low air excess coefficients result in a decrease in combustion temperature. Furthermore, as the coefficient increases, the uniformity of the temperature field also improves. Excessively high air excess coefficients significantly elevate NOx concentrations, adversely impacting the environment. Consequently, to optimize the ladle baking process, this study recommends setting the air excess coefficient to 1.05. This is crucial for optimizing the baking process, enhancing baking efficiency, and conserving energy.

Key words*: ladle preheating; excess air coefficient; numerical simulation; energy saving; process parameter optimisation*

1. Introduction

Regenerative combustion is widely used in the steelmaking industry to heat industrial furnaces, effectively increasing the temperature of the furnace lining [1-3]. Prior to receiving molten steel, the ladle undergoes a preheating process, which not only removes moisture but also ensures that the molten steel attains the desired temperature and quality during casting [4, 5]. The evaluation of ladle preheating quality encompasses several critical indicators: thermal efficiency, pollutant emissions, and temperature uniformity within the ladle. The excess air factor, a vital operational parameter in ladle preheater operation, represents the ratio of actual air volume used for combustion to the theoretical air volume required [6,7]. This coefficient reflects the extent of excess air in the ladle and is a pivotal

factor influencing the indicators. Currently, the air-to-gas ratio in industrial settings is primarily set based on workers' experience, lacking assurance that the excess air factor falls within an optimal range. Consequently, investigating the relationship between various excess air coefficients and thermal efficiency, as well as NOx emissions, is crucial for conserving energy, reducing emissions in steel plants, and enhancing production efficiency.

Many researchers have carried out experimental studies related to the ladle preheating process [8]. For example, Garces et al. [9] conducted experiments on the radiation spectra of flames during ladle baking and, based on these findings, proposed a combustion diagnostic system that offers a novel approach to flame monitoring. Similarly, Hindasageri et al. [10, 11]employed infrared radiation thermography to measure the ladle, thereby obtaining the temperature distribution of the ladle and the heat flux density of the flame.

Unlike experimental methods, numerical calculations are characterized by high computational accuracy, and low cost. Moreover, data such as temperature at any moment and location can be obtained using numerical simulation methods [12,13]. Volkova et al. [14], fluid flow modeling was integrated with ladle modeling for the purpose of the study. The results indicated that preheating the air contributed to an increase in the ladle lining temperature. Literature [15-17] describes a novel steel ladle lining structure using Nano-insulating materials and numerically analyses its temperature field. The results show that this new material has excellent thermal insulation properties and can significantly extend the operating life of the ladle. Qi et al. [18]simulated the temperature field inside the ladle in both cases of air and oxygen-assisted combustion in jetted ladle, and concluded that oxygen enrichment can save a lot of energy.–Caetano et al. [19] performed an analysis of energy conversion and utilization based on a small boiler to recover part of the thermal energy remaining in the boiler exhaust gas stream. The results provide important information for simulation and practical processes, and the implementation of exhaust gas recirculation technology and thermal storage technology provide new methods for energy saving and emission reduction.

Regarding the impact of the excess air coefficient on combustion, Khodabandeh et al.[20] simulations to investigate the effects of excess air and air preheating temperature on temperature, flow rate, and efficiency within a combustion hearth cyclone passivation burner in an oil refinery setting. The findings indicate that optimal levels of excess air and preheating can enhance furnace temperature and efficiency, and the simulation results can be used to adjust the process in the field, thereby optimizing production. Su et al. [21] simulation study to investigate the impact of excess air on the combustion performance of a swirl burner in an industrial furnace. The results showed that an increase in the excess air ratio from 1.05 to 1.25 led to an enhancement in natural gas combustion, albeit accompanied by a substantial rise in NOx emissions.

The studies mentioned above were all about liner analysis, air temperature or burner construction. Comparatively, only a limited number of studies have been conducted on the impact of excess air on ladle preheating. Therefore, it is necessary to conduct a comparative study of ladle baking at different excess air factors. This analysis aims to identify an optimal excess air factor that facilitates higher combustion temperatures, enhances energy efficiency, and minimizes pollutant emissions. The influence of the excess air coefficient in the ladle preheating process is investigated by numerical simulation to provide theoretical support for process optimization of regenerative ladle preheaters. This research focuses on the regenerative ladle preheater, utilizing ANSYS Fluent 2024 R1 software to establish a regenerative preheating heat transfer model. The coupled heat transfer

involving combustion, flow, and ladle lining during baking was examined at different excess air coefficients. The aim is to gain a deeper understanding of the preheating process and to optimize the parameters for energy efficiency and cost reduction.

2. Numerical model and computational scheme

2.1. Physical model and their meshing

Figure 1 shows the thermal storage ladle model and its mesh. In particular, Fig.1 (a) shows a simplified schematic of a thermal regenerative ladle, including the ladle cover, burner, flow domain and liner. The burner is a concentric circle structure. The specific dimensions and representations of the ladle are detailed in Tab. 1.Based on the established physical model, the ICEM-CFD software was employed to generate a hexahedral mesh with localized refinement in the burner area. The resultant mesh, depicted in Fig. 1(b), comprises approximately 400,000 elements.

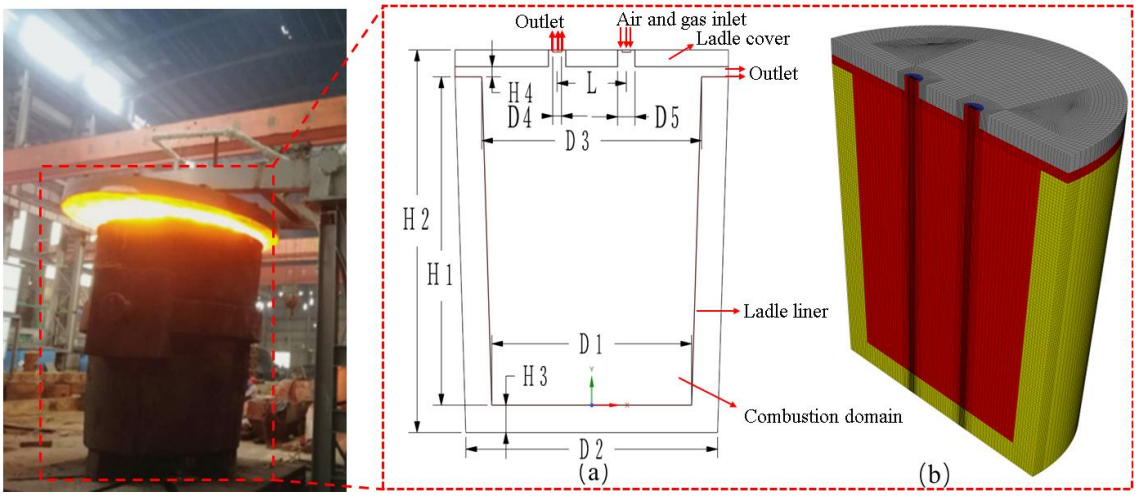

Fig. 1 Model of ladle and its mesh: (a) Model of ladle and dimensioning; (b) Meshing

Table 1 Dimensional labelling of thermal regenerative ladle

Annotate	Hidden meaning	Value [mm]
H1	Combustion domain height	3720
H2	Overall height of ladle	4335
H3	Tundish lining thickness	310
H4	Flue gas free outlet	115
D1	Inner diameter of combustion chamber bottom	2310
D2	Outer diameter of ladle bottom	2910.5
D3	Inner diameter of ladle opening	2540
D4	Burner inner diameter	100
D5	Burner outer diameter	200
L	Spacing between two burners	800

2.2. Governing equations of the model

The study includes coupled heat transfer between combustion, turbulent flue gas flow, and ladle lining during preheating. The combustion process typically coincides with gas flow, radiant heat transfer, and their mutual interactions. Among the various influencing factors, the interplay between turbulence and chemical reactions holds a paramount significance in the gas combustion process. Fluid

flow and heat transfer during the baking process are modelled by the equations for continuity (1), energy equation (2) and momentum conservation (3). Turbulence in the heat transfer process is modelled using the standard k-ε turbulence model, and Eqs. (4) and (5) give the turbulent kinetic energy and dissipation rate transport equations.[22]

$$\frac{\partial \rho}{\partial t}+\frac{\partial(\rho u_i)}{\partial x_i}=0 \tag{1}$$

$$\frac{\partial \rho T}{\partial t}+\mathrm{div}(\rho u T)=\mathrm{div}(\frac{k_1}{c_p}\mathrm{grad}T)+S_T \tag{2}$$

$$\frac{\partial \rho u_i}{\partial t}+\frac{\partial \rho u_i u_j}{\partial x_j}=-\frac{\partial p}{\partial x_i}+\frac{\partial \tau_{ij}}{\partial x_j}+\rho g_i+F_i \tag{3}$$

$$\frac{\partial \rho k}{\partial t}+\frac{\partial \rho k u_i}{\partial x_i}=\frac{\partial}{\partial x_j}[(\mu+\frac{\mu_t}{\sigma_k})\frac{\partial k}{\partial x_j}]+G_b+G_k-\rho\varepsilon-Y_M+S_k \tag{4}$$

$$\frac{\partial \rho \varepsilon}{\partial t}+\frac{\partial \rho \varepsilon u_i}{\partial x_i}=\frac{\partial}{\partial x_j}[(\mu+\frac{\mu_t}{\sigma_\varepsilon})\frac{\partial \varepsilon}{\partial x_j}]+C_{\varepsilon 1}\frac{\varepsilon}{K}(G_k+C_{\varepsilon 3}G_b)-C_{\varepsilon 2}\rho\frac{\varepsilon^2}{K}+S_\varepsilon \tag{5}$$

The one-step reaction mechanism is adopted for the combustion process. Therefore, the component transport model of Eq. (6) and the vortex dissipation concept were used to describe the chemical reaction process. In the eddy dissipation model, the chemical reaction rate is controlled by turbulent mixing and is given by the smaller of equations (7) and (8).

$$\frac{\partial \rho c_s}{\partial t}+\mathrm{div}(\rho c_s)=\mathrm{div}[D_s\mathrm{grad}(\rho c_s)]+S_s \tag{6}$$

$$R_{i,r}=(\nu''_{i,r}-\nu'_{i,r})M_{w,i}A\rho\frac{\varepsilon}{k}\min(\frac{Y_R}{\nu'_{R,r}M_{w,R}}) \tag{7}$$

$$R_{i,r}=(\nu''_{i,r}-\nu'_{i,r})M_{w,i}AB\rho\frac{\varepsilon}{k}\frac{\sum_P Y_P}{\sum_j^N \nu''_{j,r}M_{w,j}} \tag{8}$$

The radiative heat transfer during combustion is controlled by the DO (discrete ordered) radiation equation of Eq. (9).

$$\frac{dI(r,s)}{ds}+(\eta+\sigma_s)I(\vec{r},\vec{s})=\eta n^2\frac{\sigma T^4}{\pi}+\frac{\sigma_s}{4\pi}\int_0^{4\pi}I(\vec{r},\vec{s'})\phi(\vec{s},\vec{s'})d\Omega' \tag{9}$$

The media contributing to radiation within the ladle consist of the gas medium and the ladle lining. The impact of the radiative heat transfer distribution is manifested through the gas absorption coefficient. The gas radiative emissivity is determined using the WSGGM model. The governing equations for the gas absorption coefficient and the gas radiant emissivity are Eqs. (10) and (11).[23]:

$$\eta=-\left(\frac{1}{L}\right)\ln(1-\delta) \tag{10}$$

$$\delta=\sum_{i=0}^{l}\eta_{\varepsilon,j}(T)\left(1-e^{-k_i pL}\right) \tag{11}$$

2.3. Boundary conditions and solving method

Boundary condition settings play a crucial role in the numerical simulation of the ladle preheating process. The boundary conditions are defined as follows:

(1)Inlet Boundary Conditions: Velocity inlet boundary conditions are employed for the inlet. Tab. 2 shows the composition of the converter gas with a calorific value of 7413 kJ/Nm^3, a

temperature of 310 K and a flow rate of 0.22 m³/s. Tab. 3 shows the physical parameters of the ladle refractory and the gas. Tab. 4 shows the excess air coefficient (α) and air flow rate at a temperature of 1073 K.

Table 2 The main components of converter gas (volume concentration)

CO	CO_2	H_2	N_2	O_2	H_2O
60.2%	14.6%	1%	18%	0.2%	5.7%

Table 3 Setting of physical properties of refractory materials and gases

Physical property	Coke oven gas	Refractory material
Thermal conductivity [W m^{-1} K^{-1}]	volume-weighted-mixing-law	5.314-0.00337T
Specific heat [J kg^{-1} K^{-1}]	mixing-law	803+0.000618T
Density [kg m^{-3}]	mass-weighted-mixing-law	2860

Table 4 Combustion gas flow rate at different air excess coefficients

Batch number	Excess air coefficients	Flow rate [m^3/s]
Group 1	0.9	0.2914
Group 2	1.0	0.3238
Group 3	1.1	0.3562
Group 4	1.2	0.3886

(2) Outlet boundary conditions: The gap between the ladle cover and the ladle is set as the pressure outlet boundary. The flue gas burner outlet is an air and gas passage and is set to a pressure outlet boundary of -200 Pa.

(3) Other boundary conditions: Coupled walls are employed for intersecting walls. The outer wall of the ladle is presumed to be adiabatic. The combustion domain and the initial temperature the ladle is both assumed to be 1030 K. The gravitational acceleration is taken as 9.8 m/s²; and the operating pressure is atmospheric, specifically 101,325 Pa.

The SIMPLEC algorithm was used to solve the model equations. The preheating is simulated for 3600 s and the commutation time of the regenerative combustion is 30 s. During the transient calculation phase, an adaptive time step is initially utilized, followed by a fixed step size of 0.125 seconds once the residuals stabilize. This adjustment serves to expedite the computation without compromising precision.

3. Simulation results and analysis

3.1. Mesh validation and model validation

(1) Meshing Validation: The objective of grid-independence validation is to ascertain whether the physical quantities of interest exhibit substantial variations as the mesh density increases. In this study, three meshing strategies are employed for grid-irrelevance validation, namely, 200,000 for a coarse mesh, 400,000 for a medium mesh, and 700,000 for a fine mesh. By selecting an excess air coefficient of 1.1, the temperature at the longitudinal centerline of the ladle was monitored, with the results depicted in Fig.2 (a). The results show that the temperature change curves by the three meshes exhibited essentially the same trend. T The coarse mesh exhibited the lowest temperatures, with a temperature difference of 15 ℃ compared to the others. The discrepancy between the medium and fine meshes remained within 5 ℃. To enhance computational efficiency, the number of 400 000 mesh was chosen as the computational grid for all scenarios.

(2) Model Validation: The numerical model designed in the previous section is validated by the data monitored in the field in literature [24]. Both the ladle model and boundary conditions use the data given in the literature. A schematic of the temperature monitoring points is shown in Fig.2 (b). The distances of the monitoring points from the bottom of the ladle were 100 mm, 700 mm, 1800 mm and 3000 mm. The results of the comparison between the simulated and measured values are shown in Tab. 5. Difference value between measured and calculated value, calculated as follows: Difference value = (Measured value - Analogue value) / Analogue value * 100%. The relative error of the temperature at monitoring point 3 is too large, which may be due to a shift in the actual flame, inaccurate thermocouple monitoring or inaccurate monitoring position. The rest of the errors are less than 5%, and it can be considered that the error in the model calculation is within the permissible range. Therefore, the model established in this paper can be used for the simulation study of the current ladle roaster.

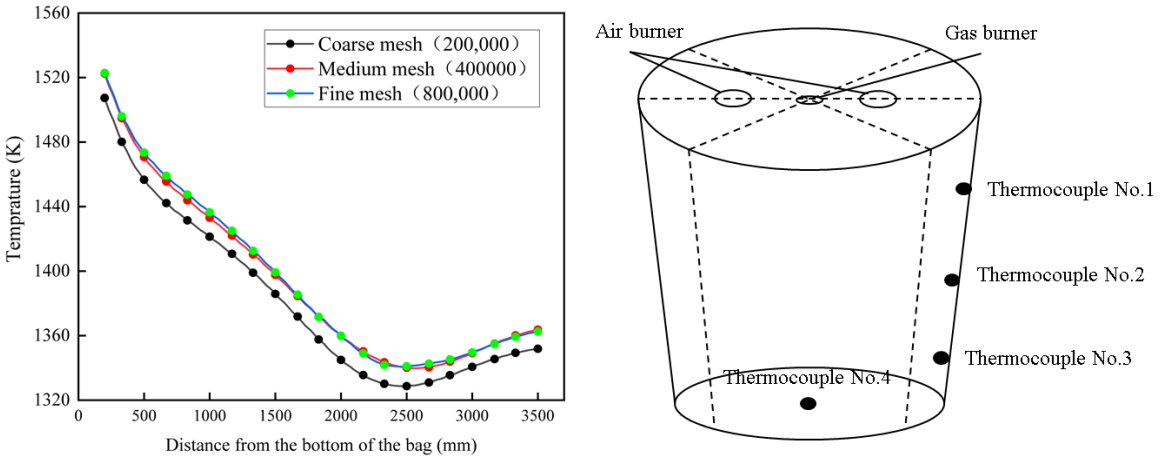

(a) (b)

Fig.2 Verification of grid irrelevance and site monitoring point map: (a) Comparison of temperatures at the centre axis in the height direction; (b) Schematic of thermocouple points

Table 5 The measured values and the simulated values

Monitoring point	No. 1.	No. 2.	No. 3.	No. 4.
Measured value [K]	1383	1432	1485	1558
Analog value [K]	1348	1371	1406	1551
Relative differences [%]	-2.5	-4.3	-5.3	0.44

3.2. Characteristics of fluid flow in the ladle

The state of gas flow in the ladle significantly influences temperature uniformity and indirectly the formation of NOx. Figures 3(a)-(g) depict the gas flow state inside the ladle at the end of the baking, with cross-sections located at 100 mm, 1700 mm, and 3500 mm from the bottom, respectively. In figure, gas and air form a jet after being injected at high speed in the right burner. Initially it is able to remain stable, but as it mixes and burns, the structure changes. The high-temperature flue gas resulting from combustion directly impacts the ladle bottom and disperses in all directions upon encountering resistance from the lining. As the flue gases ascend back to the top, a cyclonic flow is generated, drawing a significant quantity of high-temperature flue gases towards the ladle bottom. This state of affairs affects the stability and completeness of the combustion process, thus reducing NOx emissions. As the excess air coefficient increases, the gas flow performance increases, but the

degree of reflux decreases. The burner on the left side carries out flue gas recovery to improve the utilisation of waste heat. The cyclonic flow generated in the ladle helps to extend the residence time of the high-temperature flue gases, creating a low-oxygen environment for high-temperature, low-oxygen combustion, thus improving heat utilisation.

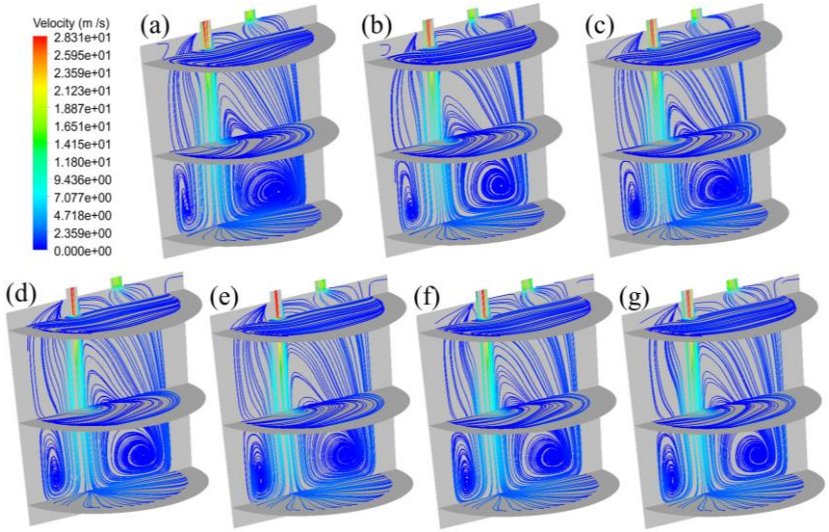

Fig.3 Flow line diagram of ladle cross-section with different air excess coefficients: (a)α=0.9; (b)α=0.95; (c)α=1; (d)α=1.05; (e)α=1.1; (f)α=1.15; (g)α=1.2

Figure 4 depicts the lateral velocity variation curves of the ladle at various heights. In all instances, the velocity decreases abruptly near the inner wall of the ladle. At a height of 100 mm from the bottom of the ladle, the velocity first increases and then decreases on both sides of the flame. Conversely, at 1700 mm, the velocity decreases initially and then increases on both sides of the flame. At 3500 mm, the velocity remains almost constant. At the bottom of the ladle it shows that a large coefficient is associated with a large velocity, but in the middle and top of the ladle there is no pattern.

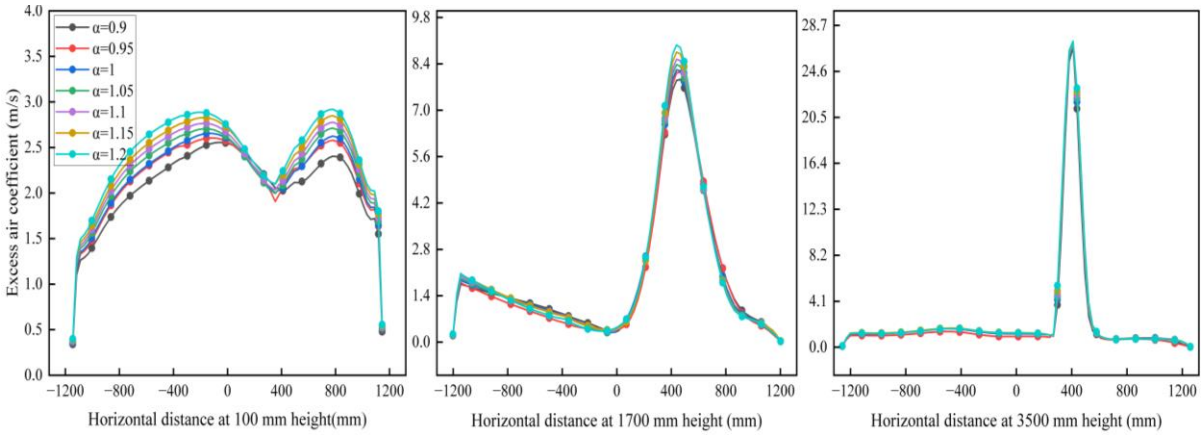

Fig.4 Flow line diagram of ladle cross-section with different air excess coefficients: (a)α=0.9; (b)α=0.95; (c)α=1; (d)α=1.05; (e)α=1.1; (f)α=1.15; (g)α=1.2

3.3. Different excess air coefficient temperature distributions in the ladle

By conducting combustion simulations of the regenerative ladle Preheater, a temperature field cloud of the ladle cross-section was obtained, as illustrated in Figures 5(a)-(g). In these diagrams, air and gas are mixed and combusted, releasing a substantial amount of heat energy and generating high-temperature flue gases. These gases undergo heat exchange and reach the ladle's bottom, where their

temperature decreases. Subsequently, the flue gas spreads along the bottom towards the ladle wall. Observation of the flame reveals that the peak temperature occurs on the flame's exterior. The temperatures on both sides of the flame exhibit a trend of initial decrease, followed by an increase, and a final decrease. As the excess air coefficient increases, the area of the high-temperature zone above 1430 K initially expands and then contracts. This is due to the fact that at excess air coefficients less than 1, the amount of air is lower than the theoretical value, making the combustion reaction incomplete and the heat release incomplete. At coefficients greater than 1, a large amount of air carries away some of the heat. At the flue gas outlet, a localised low temperature occurs, but the area gradually decreases. This is due to the fact that the excess air factor is too small and combustion produces less flue gas, thus making the pressure inside the packet lower than the external pressure, leading to the entry of air, which lowers the temperature. The flame is deflected under the action of the swirling flow. This is due to the fact that when the smoke produced by the flame encounters the wall of the ladle; the flow is restricted, thus forcing the flame to flow along the wall of the ladle, resulting in the offset of the flame. At the same time, the extent of the jet's coiling suction of the smoke in the right-hand region is less than that in the left-hand region, creating a situation where the right-hand side is less than the left-hand side pressure

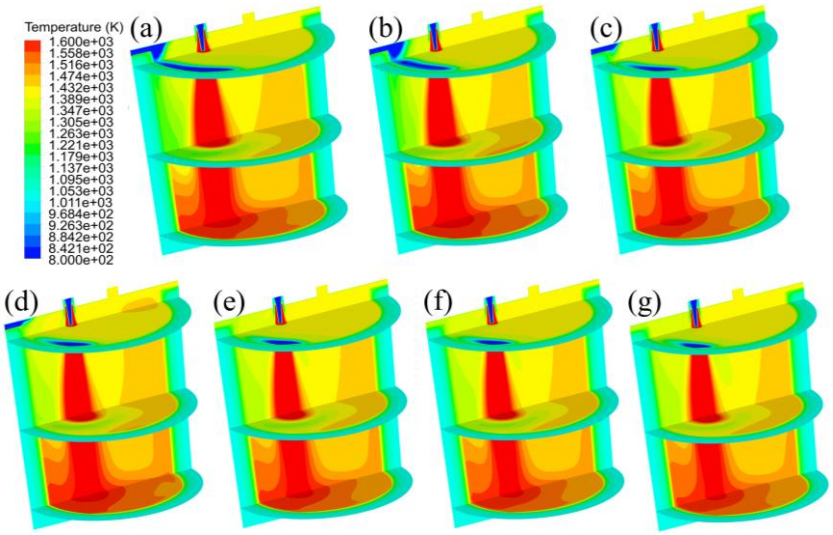

Fig. 5 Temperature distribution of ladle with different air excess coefficients: (a)α=0.9; (b)α=0.95; (c)α=1; (d)α=1.05; (e)α=1.1; (f)α=1.15; (g)α=1.2

Figure 6 depicts the distribution of maximum and average temperatures within the ladle. In the graph, as the excess air coefficient increases, the maximum temperature occurs at a coefficient of 1.05, where the maximum temperature rises from 2400.3 K to 2430.82 K and then decreases to 2334.69 K. The average temperature, on the other hand, remains essentially unchanged after it rises from 1390.52 K to 1405.73 K. The average temperature is also shown in the graph, where the average temperature is shown in the graph. Before the coefficient is less than 1.05, with a gradual increase in the amount of air, the fuel is able to obtain enough oxygen for complete combustion, thus releasing more heat and thus increasing the combustion temperature. As the coefficient increases further, too much air leads to an increase in the amount of exhaust gases. The exhaust gases carry away a large amount of heat, thus lowering the temperature of the combustion chamber.

Figure 7 depicts the distribution of average temperature around the circumference of the ladle at different heights. The average temperature around the circumference of the ladle decreases with

increasing distance from the bottom. The temperature variation starts to stabilise at a distance of more than 2000 mm from the bottom, with a more pronounced decrease at 3000 mm. This is due to the fact that beyond a certain height, direct convective heat transfer from the bottom decreases and radiative heat transfer dominates. As the coefficients increase, the temperature difference between the upper and lower parts are 169.9 K, 167.2 K, 159.7 K, 146.9 K, 143.8 K, 145.1 K, and 140.6 K. The overall temperature difference is becoming smaller, and the homogeneity of the temperature field is gradually increasing.

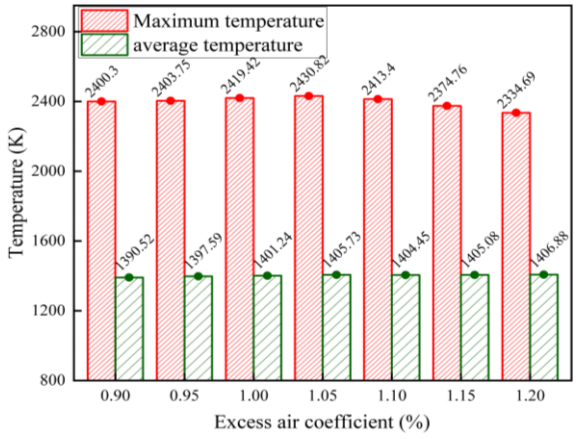

Fig. 6 Ladle maximum and mean temperatures

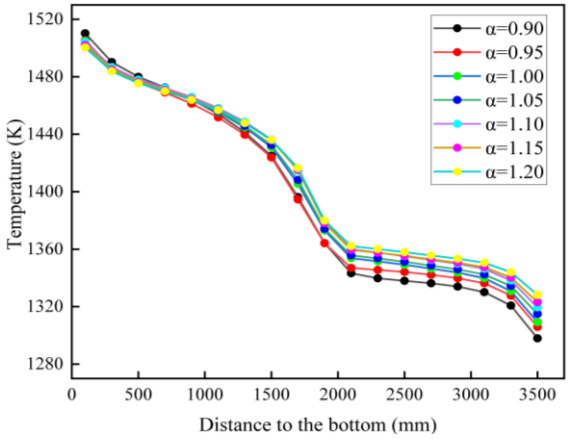

Fig. 7 Average circumferential temperature

3.4. Distribution characteristics of the pollutant NOx

The NOx produced in combustion is mainly of the thermal. Its generation is influenced by factors such as fuel composition, combustion temperature, and residence time within the high-temperature zone. Among these factors, temperature plays a pivotal role [26].

Figure 7 depicts the temperature field at α = 1.1 and the distribution of NOx concentration at different coefficients. Comparing the figure temperature field cloud with the NOx concentration distribution figure, it can be found that the distribution of NOx in the ladle is temperature dependent and the concentration increases gradually with increasing temperature. The highest concentration occurs in the middle part of the flame. This is because the production of NOx requires the presence of nitrogen, oxygen and high temperature. At the inception of the combustion reaction, despite adequate oxygen concentration, the temperature remains low, rendering the reaction challenging to initiate. Conversely, during the midpoint of the reaction, both high temperature and adequate oxygen conditions are met, leading to increased NOx production. When the coefficient is less than 1.05, the NOx concentration progressively rises with increasing coefficients; however, a slight decline is observed at α = 1.2. The distribution of NOx is not uniform due to the flow field, with higher NOx concentrations in the centre of the flame, the bottom of the ladle and the near-wall region, which is essentially the same as the temperature field distribution. This also shows that the ambient temperature and the length of time the flue gas is in the furnace have a great influence on the production of NOx.

Figure 8 depicts the variation in average NOx concentration at the flue gas outlet and in the combustion domain. The NOx concentration in the outlet and combustion domains increases significantly with increasing excess air factor, but a decrease in concentration in the combustion domain occurs at α = 1.2, which is consistent with the results of the cross section in Fig. 8. This is due to the fact that the increase in air content leads to an increase in oxygen content and an increase in NOx concentration, but when the coefficient is too large, the effect of temperature is more significant

and the temperature decreases, leading to a decrease in NOx concentration. In conclusion, NOx production is affected by oxygen concentration and temperature, and a moderate excess air coefficient will increase the furnace temperature and reduce NOx concentration.

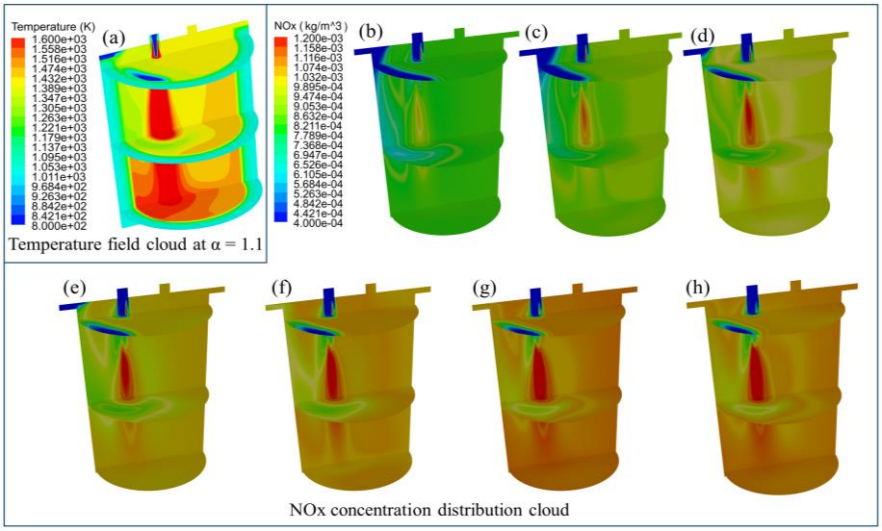

Fig. 7 Temperature field at α = 1.1 and NOx concentration distribution at different coefficients: (a) Temperature field at α = 1.1; NOx concentration :(b)α=0.90; (c)α=0.95;(d)α=1; (e)α=1.05; (f)α=1.1; (g)α=1.15; (h)α=1.2

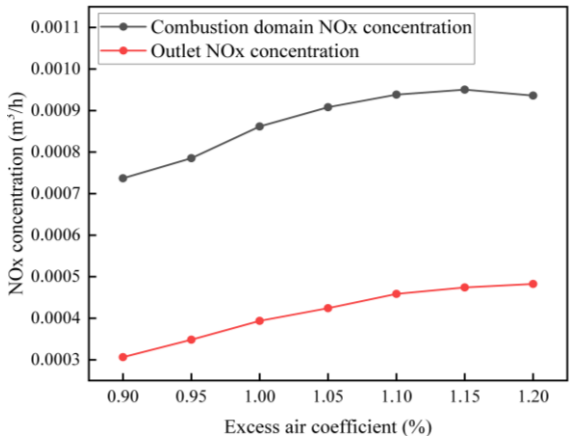

Fig. 8 Curves of average NOx concentration changes at the flue gas outlet and in the combustion domain.

4. Reach a verdict

In this study, a multi-field coupled mathematical model of gas combustion, flow and coupled heat transfer is established based on ANSYS Fluent 2023R1 with the background of a heat storage ladle. The internal flow field, temperature field and the distribution of NOx in the ladle under different excess air coefficients are also analysed and investigated to provide a theoretical basis for the control of the actual ladle preheating process. The main conclusions drawn from the analysis are as follows:

(1) Thermal storage ladle preheaters reduce flue gas emissions and increase the utilisation of flue gas waste heat. The lower excess air coefficient allows air to enter the ladle, thus creating a localised low temperature zone within the ladle.

(2) The maximum and average temperatures of the flame occur at an excess air factor of 1.05. Excess air coefficients that are too low low will result in incomplete chemical reactions and reduce the uniformity of the temperature field. Conversely, a coefficient that is too high will increase the uniformity of the temperature field, but will reduce the overall temperature.

(3) NOx generation is affected by oxygen concentration and temperature. The high temperature region is the main region for NOx generation, while in the region with lower temperature, NOx generation will be relatively low. Meanwhile, NOx concentration increases gradually with the increase of excess air factor. Therefore, an excess air factor of 1.05 is recommended, taking into account factors such as baking temperatures and reduced pollutant emissions.

(3) By simulating and analysing the heat storage ladle, it is possible to predict the appropriateness of the process parameters and reduce the research and development costs. This is of great theoretical and practical significance for energy saving and emission reduction in the preheating process of steel ladle.

Acknowledgments

This work was supported by the National Natural Science Foundation of China, under grant number 71571091 and 71771112.

Nomenclature

A, B	– empirical constants	$\vec{r}$	– position vector
c_s	– mass fraction	$R_{i,r}$	– net production rate of component i due to reaction r, [kg/(m ^{3}s)]
$C_{\varepsilon 1}$,$C_{\varepsilon 2}$,$C_{\varepsilon 3}$	– turbulence modelling constant	$\vec{s}$	– direction vector
C_p	– specific heat capacity, [J/(kg K)]	$\vec{s'}$	– scattering direction vector
D_s	– diffusion coefficient, [m ^{2}/s]	S_k, S_ε	– source term of k and ε, [kg/(m s^4)]
F_i	– volumetric force	S_T	Generated items
G_k, G_b	– turbulent kinetic energy production term	S_s	– chemical reaction rate, [kg/(L s)]
g_i	– volumetric force	t	– time, [s]
I	– radiation intensity, [W/m ^{2}sr]	T	– temperature, [K]
k_1	– heat transfer coefficient	u	– velocity vector
L	– ray length, [m]	x_i, x_j	– transmission distance, [m]
$M_{w,i}$	– Molecular weight of substance i	Y_M	– dissipative term
n	– refraction coefficient, [W/m ^{3}]	Y_P, Y_R	– mass fractions of the product and reactant
p	– pressures, [Pa]		
Greek symbols			
δ	– radiation emissivity	σ_k, σ_ε	– Prandtl number for k and ε
η	– absorption coefficient, [1/m]	σ_s	– scattering coefficient, [1/m]
ρ	– density, [kg/m^3]	$v''_{i,r}$, $v'_{i,r}$	– stoichiometry of products and reactants
μ	– molecular turbulent, [Pa s]	Φ	– phase function
μ_i	– velocity component, [m/s]	Ω'	– steradian angle, [sr]
μ_t	– viscosity, [Pa s]		
τ_{ij}	– stress tensor		

Reference

[1] Gaber,C., *et al*., An experimental study of a thermochemical regeneration waste heat recovery process using a reformer unit, *Energy.*, 155(2018), pp. 381-391.
[2] El-Behery,S. M., *et al*., Performance evaluation of industrial glass furnace regenerator, *Energy*., 119(2017), pp. 1119-1130.
[3] Yuan,F., *et al*., Heat transfer performances of honey-comb regenerators with square or hexagon cell opening, *Applied Thermal Engineering.*, 125(2017), pp. 790-798.
[4] Chaikin,B. S., *et al*., State-of-the-art plants for drying and high-temperature heating of ladles, *Refract Ind Ceram.*, 47(2006), 5, pp. 283–287.
[5] Liu,Y., *et al*. A Review of Physical and Numerical Approaches for the Study of Gas Stirring in Ladle Metallurgy, *Metallurgical and Materials Transactions B.*, 50(2019), pp. 555–577.
[6] Jiang,Y., *et al*. Modelling the Mechanism of Sulphur Evolution in the Coal Combustion Process: The Effect of Sulphur–Nitrogen Interactions and Excess Air Coefficients, *Processes*., 11(2023), 5, pp. 1518.
[7] Hao,X. Y., *et al*. Experimental and simulation analysis of the performance of premixed vertical ejectors, *Applied Thermal Engineering.*, 250(2024), pp. 123527.
[8] Semakhin,W., Vyal'shina,L. E., Optimizing the Drying and High-Temperature Heating of the Lining of Steel-Pouring Ladles, *Metallurgist.*, 48(2004), 5,pp. 275-278.
[9] Garces,H. O., *et al*. Radiation measurement based on spectral emissions in industrial flames, *Measurement.*, 87(2016), pp. 62–73.
[10] Hindasageri,V., *et al.*, Heat transfer distribution for three interacting methane–air premixed impinging flame jets, *International Journal of Heat and Mass Transfer*., 88(2015), pp. 914–925.
[11] Glaser,B., *et al.*, Thermal Modelling of the Ladle Preheating Process, *Steel Research International*., 82(2011), 12, pp. 1425–1434.
[12] Yuan,F., *et al*., Combustion performance of nozzles with multiple gas orifices in large ladles for temperature uniformity, *Journal of Iron and Steel Research International*., 25(2018), pp. 387-397.
[13] Volkova,O., Janke,D., Modelling of temperature distribution in refractory ladle lining for steelmaking, *ISIJ International*., 43(2003), 8, pp. 1185-1190.
[14] Volkova,O., *et al.*, Ladle Heating Procedure and Its Influence on the MgO–C-Oxidation, *Materials and Manufacturing Processes*., 23(2008), 8, pp. 758–763.
[15] Sun,Y.,*et al*., Numerical simulation of thermal insulation and longevity performance in new lightweight ladle, *Concurrency and Computation: Practice and Experience*., 32(2020), 22.
[16] Li,G. F., *et al*., Numerical simulation of temperature field and thermal stress field in the new type of ladle with the nanometer adiabatic material, *Advances in Mechanical Engineering.*, 7(2015), 4.
[17] Gruber,D., Harmuth,H., Thermomechanical behavior of steel ladle linings and the influence of insulations, *Steel Res Int.*, 85(2013), 4, pp. 512-518.
[18] Qi,F. S., *et al*., Numerical study on ladle preheating process of oxy-fuel combustion, *Thermal Science.*, 24(2020), 6, pp. 3511-3520.
[19] Caetano,N. R., et al., Energy Recovery Based on Exhaust Gas Recirculation and Heat Regeneration Processes Applied in a Firewood Boiler, *Journal of Engineering Thermophysics*., 32(2023), 3, pp. 482-501.
[20] Khodabandeh,E., et al., Effects of excess air and preheating on the flow pattern and efficiency of the radiative section of a fired heater, *Applied Thermal Engineering*, 105(2016), pp. 537-548.
[21] Su,Y., et al., Combustion Performance and NO Emission in Industrial Furnace under Preheated Air Condition with Different Excess Air Ratio, *Advanced Materials Research*, 402(2011), pp. 463 - 466.
[22] Khoshhal,A., *et al*., The CFD Modeling of NOx Emission, HiTAC and Heat Transfer in an Industrial Boiler, *Numerical Heat Transfer, Part A: Applications.*, 58(2010), 4, pp. 295–312.
[23] Park,S., *et al*., Effects of gas and particle emissions on wall radiative heat flux in oxy-fuel combustion, *J Mech Sci Technol.*, 26(2012), pp. 1633–1641.
[24] Ji,L. L., *et al*., Numerical simulation on preheating system of regenerative ladle, *Iron and Steel*., 48(2013), 4, pp. 76-81. (In China)

Submitted: 05.10.2024.
Revised: 25.11.2024.
Accepted: 26.11.2024.